LUND UNIVERSITY

Exploration of Supraventricular Conduction with respect to Atrial Fibrillation. Methodological Aspects on Selected Techniques

Carlson, Jonas

2005

Europace (2005) 7, S39–S48

ELSEVIER

EUROPEAN SOCIETY OF CARDIOLOGY®

Can orthogonal lead indicators of propensity to atrial fibrillation be accurately assessed from the 12-lead ECG?

Jonas Carlson [a,*], Rasmus Havmöller [a], Alberto Herreros [b], Pyotr Platonov [a], Rolf Johansson [c], Bertil Olsson [a]

[a] *Department of Cardiology, Lund University, Sweden*
[b] *Department of Automatic Control, University of Valladolid, Spain*
[c] *Department of Automatic Control, Lund University, Sweden*

Submitted 13 January 2005, and accepted after revision 28 April 2005
Available online 28 July 2005

KEYWORDS
P-wave;
12-lead ECG;
orthogonal VCG;
inverse Dower transform

Abstract **Aims** When analyzing P-wave morphology, the vectorcardiogram (VCG) has been shown useful to identify indicators of propensity to atrial fibrillation (AF). Since VCG is rarely used in the clinical routine, we wanted to investigate if these indicators could be accurately determined in VCG derived from standard 12-lead ECG (dVCG).
Methods ECG and VCG recordings from 21 healthy subjects and 20 patients with a history of AF were studied. dVCG was calculated from ECG using the inverse Dower transform. Following signal averaging of P-waves, comparisons were made between VCG and dVCG, where three parameters characterizing signal shape and 15 parameters describing the P-wave morphology were used to assess the compatibility of the two recording techniques. The latter parameters were also used to compare the healthy and the AF groups.
Results After transformation, P-wave shape was convincingly preserved. P-wave morphology parameters were consistent within the respective groups when comparing VCG and dVCG, with better preservation observed in the healthy group.
Conclusion VCG derived from routine 12-lead ECG may be a useful alternate method for studying orthogonal P-wave morphology.

* Corresponding author. Department of Cardiology, EA15, Lund University Hospital, SE-221 85 Lund, Sweden. Tel.: +46 46 177041; fax: +46 46 157857.
E-mail address: jonas.carlson@med.lu.se (J. Carlson).

1099-5129/$30
doi:10.1016/j.eupc.2005.04.012

Introduction

The mechanisms responsible for initiation and maintenance of atrial fibrillation (AF) are increasingly better understood. Following the identification of anatomic origin of the ectopic P-waves triggering the arrhythmia [1], interventions targeted against this mechanism clearly verify the role of a trigger factor in the development of paroxysmal AF.

Multiple studies have verified that the propensity for paroxysmal AF is linked not only to the occurrence of a trigger factor, but in addition also to widening of the P-wave recorded during sinus rhythm, representing evidence of a vulnerable arrhythmia substrate. The P-wave widening may, however, be subtle and is not a mandatory prerequisite for identification of patients prone to paroxysmal AF. In fact, the morphology of the orthogonally recorded P-waves differed significantly between patients with paroxysmal AF and arrhythmia-free healthy control subjects, within normal P-wave duration, suggesting a deterioration of the inter-atrial conduction across the infero-posterior part of the inter-atrial septum [2]. This mechanism was verified in invasive studies [3,4], further explaining the earlier observed P-wave changes.

Orthogonal ECG leads are seldom recorded in the clinical routine. However, since the morphology of the QRS-complexes in orthogonal leads can be reconstructed by recalculation from standard 12-lead ECG signals [5], we have explored the possible reconstruction of the orthogonal P-waves for identification of morphological changes associated with AF.

Methods

Study population

Twenty-one healthy volunteers and 20 patients with a history of AF were enrolled in the study. The healthy group contained 10 women and 11 men with median age of 56 years and the AF group five women and 15 men with median age 69.5 years.

The study complies with the Declaration of Helsinki and all subjects gave informed consent to participate in the study. The study was approved by the local ethics committee at Lund University, approval numbers LU 325-00 (healthy group), and LU 207-99, LU 394-03, and LU 31-03 (AF group).

ECG and VCG recordings

For each subject, standard 12-lead ECG (ECG) and Frank-lead VCG (VCG) were recorded. Both recordings were 6 min in length and performed immediately after each other with the subjects at rest. The recordings made from the AF group were performed during verified sinus rhythm. Data acquisition was made at a sampling speed of 1000 samples per second and channel, with the resolution 0.625 μV using custom made hardware and software (Siemens—Elema, Sweden). For subsequent analyses, data were transferred to a GNU/Linux workstation.

Data preprocessing

All data analyses were performed using custom made software running on MATLAB R13 (www.mathworks.com). Both ECG and VCG recordings were transformed into the WFDB format used by PhysioNet [6], in this process the ECG recordings were also converted to orthogonal signals (dVCG) using the inverse Dower transformation [5]. The transformation is described in the first section and an error analysis in the second section of the Appendix.

Power line interference was removed using a 50 Hz bandstop filter. Baseline wander was removed by using a lowpass filter at 0.5 Hz to calculate the baseline and then subtracting it from the signal.

Extracting P-waves

As in most ECG and VCG analyses, the first step was an automated detection of the QRS-complexes [7]. Based on their morphology, all QRS-complexes were then sorted into different groups, where the first group was created simply by taking the first QRS-complex of the recording. The following QRS-complexes were then compared with this group and added to it provided they had similar morphology or otherwise used to create a new group with different morphology. When more than one group was found, the following QRS-complexes were put in the group with the most similar morphology. To define whether two morphologies were similar or not, correlation function analysis was used, where a correlation coefficient greater than 0.9 was used to define similarity.

When all QRS-complexes had been assigned to a group, the average morphology of each group was calculated. Each QRS-complex in the individual groups were then time-shifted and compared with the group's average and adjusted to create

the highest correlation. The average morphology of each different group was then recalculated. For each group of QRS-complexes, onset and end of the group's average morphology could be corrected manually in order to produce the most accurate value for later calculation of PQ-time.

In this study, to extract P-waves, only QRS-complexes belonging to the group with the largest number of complexes were used. P-wave extraction was made by defining 250 samples wide signal windows immediately preceding each QRS-complex, in which the P-wave was believed to be located. If cases with unusually long PQ-time or P-wave duration were found, both length and position of the signal window could be altered in order fully to cover the P-wave.

Groups of signal windows with different morphologies were then created using the same technique as with the QRS-complexes described above. Using the morphology of the different groups, the actual P-waves were defined by manual setting of onset and end. The amplitude at the onset of the P-wave was subtracted from the signal to create a baseline value of 0.

Fig. 1 shows an example of the noise reducing effect of P-wave signal averaging.

In the subsequent comparisons between recording techniques and between healthy subjects and those with history of AF, only the group with the largest number of P-waves was used, and only the signal between onset and end of the P-wave.

Mathematical comparison of P-waves

Comparisons were made between VCG and dVCG P-wave morphologies in each study subject. First, the signal-averaged P-waves were adjusted in length and time-shifted to achieve the highest correlation coefficient in order to compensate for differences in settings of onset and end. Second, an ordinary least-squares estimation of the residual in each individual lead was performed to minimize differences in amplitude (see Appendix, last section).

The parameters used to compare P-waves mathematically were the maximum correlation coefficient, the scaling parameter obtained from the least-squares minimization of the residual, and the residual error. Values were calculated for each individual lead.

Comparing P-wave morphology parameters

Before analysis of numerical P-wave morphology parameters, noise was removed from the P-waves by applying a 5-term simple moving average filter. The filter was applied repeatedly until no local maxima were found in the signals, closer than 20 ms.

In order to analyze just the temporal behaviour of the P-wave, regardless of its spatial direction, a vector magnitude was calculated as:

$$SM = \sqrt{X^2 + Y^2 + Z^2}$$

Several parameters were used to describe the P-wave morphology. General parameters were P-wave duration and PQ-time. In lead X, location and amplitude of maximum is X_{max}. In lead Y, location and amplitude of maximum is Y_{max}. In lead Z, location and amplitude of minimum is Z_{min}, location of first zero-crossing after the minimum is Z_{zero}, duration from zero-crossing to end is Z positive phase, Z_{pos}, location and amplitude of the maximum located after the zero-crossing is Z_{max}, and difference between the amplitudes of Z_{max} and Z_{min}. In SM, the parameters were the minimum before the P-wave end (nadir) and the distance, in ms, between the two most prominent maxima (Z_{diff}, if present). See Fig. 1 for an illustration of these parameters.

The values of P-wave duration and PQ-time were obtained from the manual settings of QRS and P-wave onset and end, while all morphology parameters were calculated by the software.

Statistics

The following statistical tests were used:

- Paired comparisons of parameters obtained from different recordings of the same subject were made using Wilcoxon's signed rank test for paired samples.
- Comparisons of parameters obtained from the two different groups were made using Wilcoxon's rank sum test.
- Comparison between the least-squares factor and the scalar 1 was made using Wilcoxon's signed rank test.

Comparisons resulting in a *P*-value less than 0.05 are denoted as significant, and those with *P*-values just above 0.05 are denoted as trends.

Results

Mathematical comparison of P-waves

The correlation coefficient obtained by comparing VCG and dVCG is shown in Table 1 and Fig. 3. The

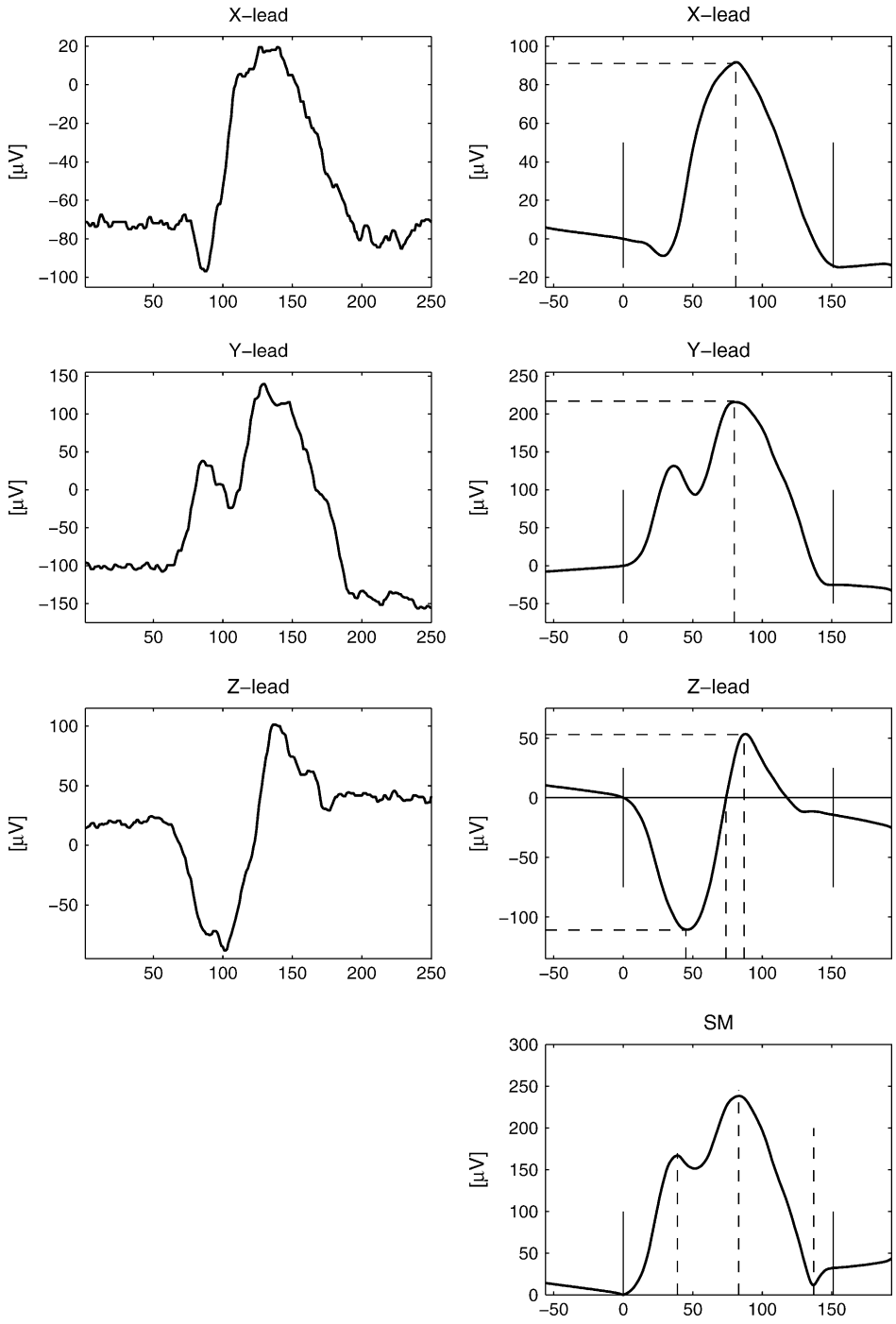

Figure 1 Example of orthogonal P-waves during one cardiac cycle (left column), and after signal averaging and calculation of SM (right column). Parameters used to describe P-wave morphology are indicated with dashed lines. In X-lead: location and amplitude of maximum is X_{max}; Y-lead: location and amplitude of maximum is Y_{max}; Z-lead: location and amplitude of minimum is Z_{min}, location of zero-crossing after minimum is Z_{zero}, and location and amplitude of maximum after zero-crossing is Z_{max}; SM: location of two peaks used to calculate interpeak distance (SM_{diff}), and location of the minimum before P-wave end (nadir). Solid lines indicate P-wave onset and end. Note the different amplitude scales.

figure indicates that 0.8 appears a suitable value to discriminate between recordings that can be defined as similar and those that cannot. Choosing 0.8, the difference in correlation between VCG and dVCG in three healthy and two AF cases would be too big to accept them as interchangeable.

The scaling parameter is also shown in Table 1. When combining all 41 cases, the values of leads X

Table 1 Mathematical comparison between P-waves from VCG and dVCG

	Healthy	AF
Correlation		
Lead X	0.95 (0.82—1.00)	0.95 (0.61—1.00)
Lead Y	0.95 (0.66—1.00)	0.95 (0.80—0.99)
Lead Z	0.92 (0.15—0.99)	0.95 (0.76—0.99)
Least squares		
Lead X	0.88 (0.46—1.24)	0.96 (0.52—1.24)
Lead Y	1.37 (0.53—1.66)	1.32 (0.61—2.53)
Lead Z	0.92 (−0.28—1.88)	1.02 (0.74—1.33)
Residual		
Lead X	0.23 (0.06—0.49)	0.23 (0.06—0.73)
Lead Y	0.24 (0.06—0.68)	0.17 (0.06—0.48)
Lead Z	0.38 (0.12—0.91)	0.32 (0.15—0.57)

Numbers are given as median and range. AF = atrial fibrillation.

and Y were significantly different from 1 (lead X median 0.95, $P < 0.01$; lead Y median 1.34, $P < 0.01$) which suggests that the numerical values of the inverse Dower transformation matrix are not entirely satisfactory for our material.

An example of the residual error is shown in Fig. 2, and numerical values in Table 1. In 17 healthy and 14 AF cases, the largest residual error was found in lead Z.

Comparing P-wave morphology parameters

Numerical values of the P-wave parameters are shown in Table 2 and their distributions in Fig. 4.

Trends or significant differences were found in the following parameters when comparing VCG recordings with dVCG: nadir location (AF group, $P = 0.07$), X_{max} location (AF group, $P < 0.01$), Y_{max} location (AF group, $P = 0.07$) and amplitude ($P < 0.01$ in both groups), and Z_{max} amplitude (healthy group, $P = 0.06$; AF group, $P = 0.04$).

The absolute values of P-wave duration, nadir location, PQ-time, Z_{min} amplitude, and Z_{diff} amplitude were all higher in the AF group regardless of what combinations of recording techniques were used, i.e. healthy VCG or dVCG may be compared with either AF VCG or dVCG ($P \leq 0.02$ in all cases).

The trend towards higher values in the AF groups is the same in Z_{max} amplitude and Z_{pos} duration ($P \leq 0.08$ in all cases).

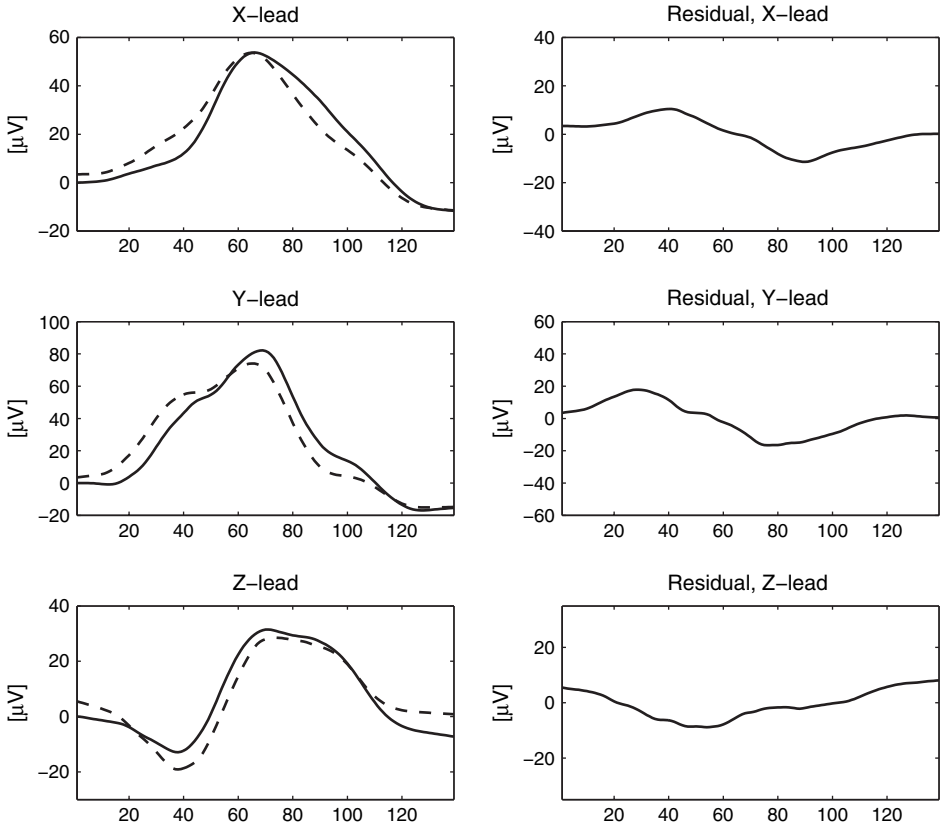

Figure 2 Typical example of signal-averaged VCG (left column, solid line), and signal-averaged dVCG calculated using the inverse Dower transformation matrix (left column, dashed line). The right column shows the residual calculated as dVCG—VCG. Note the different amplitude scales.

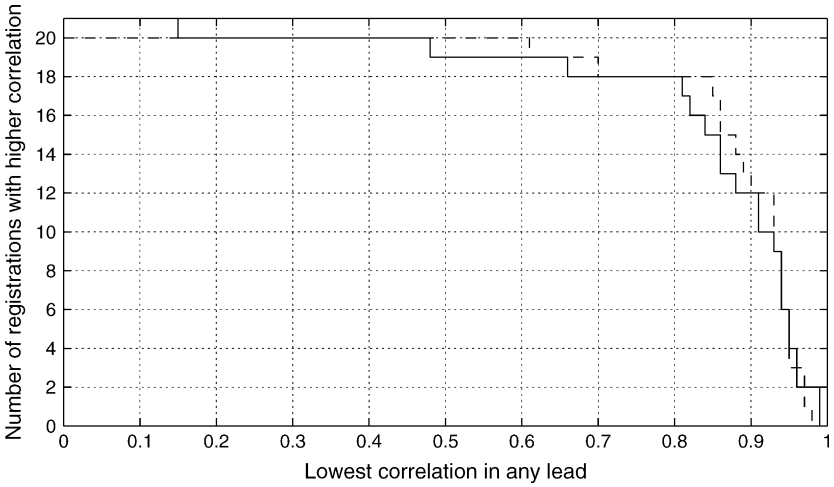

Figure 3 Comparison between VCG and dVCG by means of correlation coefficient. The figure shows in how many cases all leads have a correlation coefficient greater than a certain value. The solid line shows the healthy group, the dashed line shows the AF group.

Additional significant differences were found in X_{max} location when comparing healthy VCG with AF VCG ($P = 0.03$) and healthy dVCG with AF VCG ($P < 0.01$) and in Y_{max} amplitude when comparing healthy VCG with AF dVCG ($P < 0.01$).

In SM, a double-peaked morphology was seen in three healthy VCG, two healthy dVCG, eight AF VCG, and nine AF dVCG cases. Of these, two healthy and seven AF subjects had double-peaked SM morphology in both VCG and dVCG.

The individual differences between the parameters of VCG and dVCG, calculated as the dVCG value minus the VCG value, are shown in the Δ-columns in Table 2. Except for Y_{max} amplitude, the median values are small, which indicates that as group observations, the parameter values agree between the different recording techniques. The range of the observations is in most cases in the same order of magnitude as the value of the parameter, exceptions are P-wave duration, nadir location, and PQ-time which all have low variability.

Discussion

The first attempt to quantify the differences between the recording techniques was made using the correlation coefficient which has the advantage of being unaffected by amplitude scaling and offset. The majority of cases have a lowest correlation above 0.8. From a mathematical point of view, 0.8 may seem to be a low correlation to use for accepting two analysis results as being comparable. However, in this material a correlation of 0.8 would be a reasonable level if a physician was supposed to make equivalent interpretations of the P-wave morphology.

A least-squares compensation was performed to adjust for possible differences in amplitude scaling and offset in order to minimize the effect of these in the subsequent residual test. The scaling factor shows that the amplitude of the dVCG is higher than the VCG in lead X (scaling factor 0.95) and lower in lead Y (scaling factor 1.34). This shows that the first and second row of the inverse Dower transformation matrix in Eq. (3) (see appendix) should be adjusted by these values in order to produce a correct median amplitude in our material. The differences seen may be explained by coincidence due to small numbers or by evaluation of the original Dower matrix being made on ventricular activity [8] and evaluation of the inverse matrix being made on QRS-loops [5] rather than on high-resolution signal-averaged P-waves.

In 17 healthy and 14 AF cases, the largest residual was found in lead Z. This might be explained by lead Z having the lowest amplitude and the most complex morphology in comparison with leads X and Y. It could also, however, be a result of lead Z of a Frank-lead recording being highly dependent on information from the signal from the electrode on the back, one that is not present in the 12-lead ECG.

In a previous study [2], Frank-lead recordings of healthy subjects and patients with paroxysmal AF were used to investigate differences in P-wave morphology between the two groups.

P-wave duration and nadir location in the present study had larger values in the AF group which agrees with the previous study. The same is

Table 2 P-wave morphology parameters calculated from VCG and dVCG

	Healthy			AF		
	VCG	dVCG	Δ	VCG	dVCG	Δ
No. of P	353 (249—437)	360 (213—461)	10 (−142—100)	350 (159—462)	318 (73—462)	−9 (−195—16)
PQ-time	178 (128—213)	177 (130—212)	−2 (−16—8)	202 (157—281)	197 (155—291)	0 (−9—21)
Duration	138 (111—164)	138 (116—161)	1 (−36—12)	150 (129—221)	150 (124—235)	2 (−5—14)
Nadir	119 (94—139)	116 (95—137)	0 (−11—5)	136 (101—189)	137 (104—210)	2 (−5—21)
X_{max}						
Location	75 (55—93)	70 (55—92)	−2 (−21—11)	80 (52—134)	72 (45—124)	−6 (−43—8)
Amplitude	49 (27—81)	51 (24—79)	2 (−14—25)	46 (24—92)	52 (22—109)	−6 (−15—20)
Y_{max}						
Location	64 (47—89)	64 (47—93)	0 (−7—12)	70 (38—117)	64 (37—123)	−2 (−44—20)
Amplitude	135 (34—219)	90 (43—141)	−48 (−90—11)	103 (51—236)	80 (43—149)	−2 (−144—14)
Z_{min}						
Location	46 (15—89)	47 (32—63)	1 (−44—32)	46 (31—60)	48 (32—75)	1 (−6—16)
Amplitude	−31 (−53—−4)	−32 (−52—−10)	0 (−33—23)	−41 (−111—−23)	−48 (−144—−11)	1 (−33—40)
Z_{zero}						
Location	68 (34—106)	70 (45—111)	3 (−33—36)	76 (55—98)	76 (48—108)	2 (−30—16)
Z_{max}						
Location	91 (67—122)	86 (68—149)	−2 (−50—61)	93 (72—139)	94 (74—131)	0 (−34—19)
Amplitude	16 (2—57)	14 (5—34)	−6 (−24—20)	30 (8—63)	26 (10—44)	0 (−25—33)
Z_{pos}						
Duration	70 (15—95)	68 (16—90)	−2 (−34—30)	78 (37—123)	77 (48—127)	−2 (−16—33)
Z_{diff}						
Amplitude	50 (20—88)	50 (15—77)	−6 (−36—27)	80 (49—164)	70 (44—180)	−6 (−24—25)
SM_{diff}						
Distance	40 (36—52)	52 (50—55)	14 (14—15)	64 (40—90)	56 (28—87)	−2 (−7—15)

Values in ms except amplitudes which are μV, and the number of P-waves. The two Δ-columns show the individual differences between VCG and dVCG. Numbers are given as median and range. AF = atrial fibrillation.

true for lead Z positive phase duration although the P-values are slightly above significance. There is also agreement between the studies in the relation of double-peaked morphology in SM between healthy subjects with only few observations and those with AF where around half the group show this morphology.

A difference between the studies is found in X_{max} location which in the earlier study was found to be located later in the PAF group. In the present study this was true when comparing AF VCG with healthy VCG or dVCG but the value in AF dVCG was of the same magnitude as those in the healthy groups.

An additional observation of a difference between the studies is that the values of the parameters presented in the earlier study tended to be lower than those of the present study. This suggests that there is a possible systematic methodological difference between the two studies, for example differences in the manual settings. Another explanation may be differences in the study subjects.

The individual variation of the morphology parameters implies that although the groups' median values are low, allowing group comparisons, the ranges of these observations are large. P-wave duration, nadir location, and PQ-time have reasonably low ranges in the same order of magnitude as the precision in the manual setting of QRS and P-wave onset and end. However, the range of the parameters of location and amplitude of the different morphological points of identification may vary as much as the parameter value itself. This casts doubt whether single values should be used to define P-wave morphology, it also indicates that care should be taken when analyzing results from individual subjects.

When comparing P-waves from recorded and derived VCG in healthy individuals and those with a history of AF, we found differences that might indicate propensity for atrial arrhythmia even in

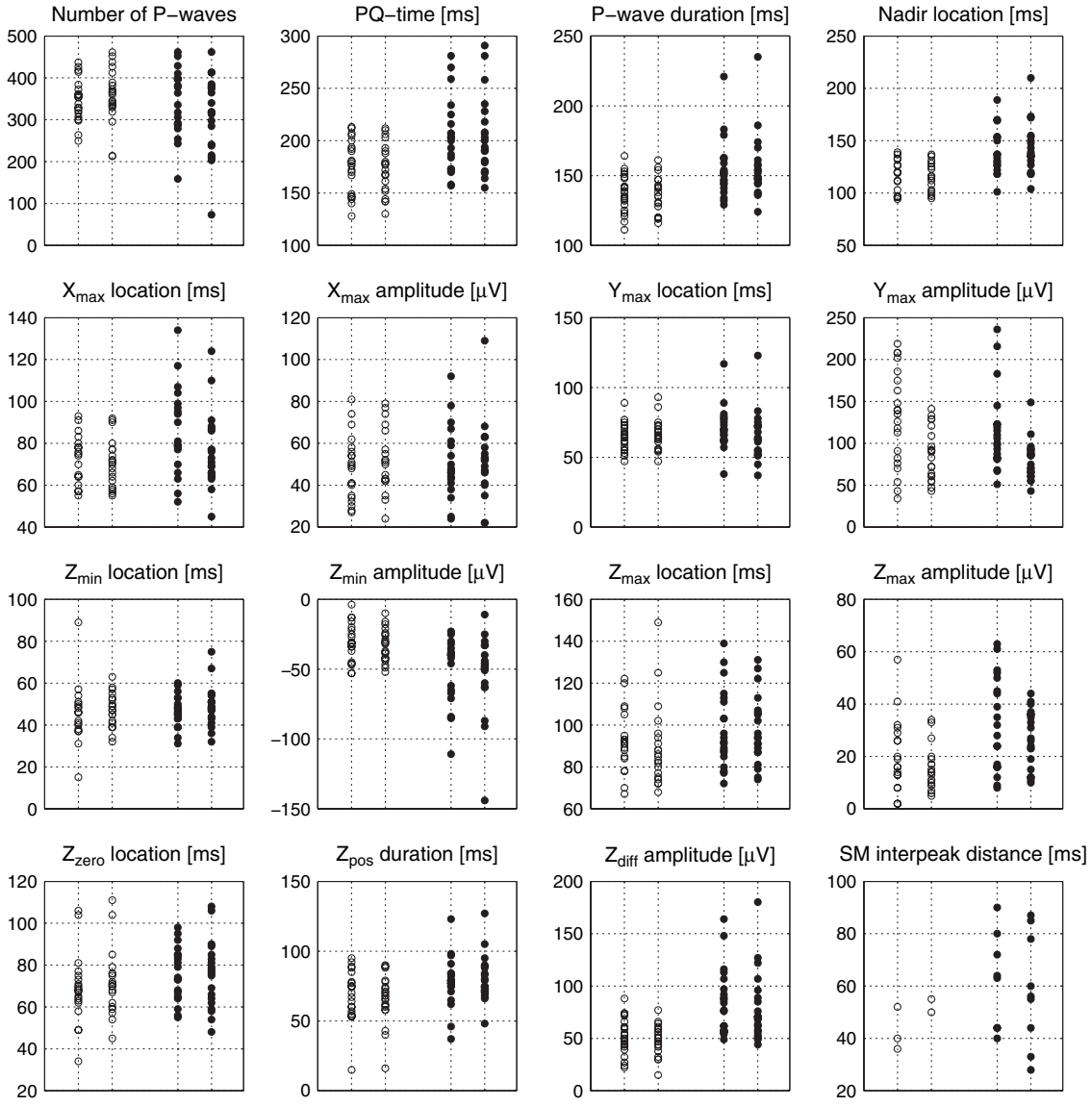

Figure 4 Distribution of the parameters used to describe P-wave morphology. In all graphs, values are from left to right: healthy VCG, healthy dVCG, AF VCG, and AF dVCG. For further information, see text.

this limited material. Our findings therefore support a future comparison in a larger, prospective, material.

Conclusions

P-waves extracted from dVCG reflect those from VCG in such a way that the morphological differences indicating propensity to AF may be identified regardless of the recording technique used.

The numerical values of the morphology parameters, however, should be used with caution, and interpretations should be made on group basis rather than individual recordings.

Acknowledgements

This study was supported by grants from the Thorsten Westerström foundation, the Franke & Margareta Bergqvist foundation and by governmental funding of clinical research within the NHS.

The authors wish to express their gratitude to Mrs. Birgit Smideberg for performing the ECG and VCG recordings.

Appendix

The inverse Dower transformation matrix

Dower et al. [8] described a method to derive 12-lead ECG from Frank-lead VCG using a transformation matrix where each lead in the ECG was expressed as a linear function of the orthogonal leads X, Y, and Z. The transformation matrix for the first eight independent leads (V_1–V_6, I, II) is:

$$D=\begin{pmatrix} -0.515 & 0.157 & -0.917 \\ 0.044 & 0.164 & -1.387 \\ 0.882 & 0.098 & -1.277 \\ 1.213 & 0.127 & -0.601 \\ 1.125 & 0.127 & -0.086 \\ 0.831 & 0.076 & 0.230 \\ 0.632 & -0.235 & 0.059 \\ 0.235 & 1.066 & -0.132 \end{pmatrix}$$

Transformation between the two lead systems is a simple matrix operation:

$$S_{ecg}=DS_{vcg} \tag{1}$$

where S_{ecg} is the ECG signal and S_{vcg} the VCG signal.

To calculate VCG from ECG we need the inverse of D but since D is non-square and therefore has no inverse, we introduce the pseudo inverse (or Moore–Penrose inverse):

$$D^{\dagger}=\left(D^{T}D\right)^{-1}D^{T}$$

The calculated VCG, $\hat{S}_{vcg}$is then:

$$\hat{S}_{vcg}=D^{\dagger}S_{ecg}=D^{\dagger}DS_{vcg}=\left(D^{T}D\right)^{-1}D^{T}DS_{vcg}=S_{vcg} \tag{2}$$

where $D^{\dagger}$ is the inverse Dower transformation matrix, with the numerical values:

$$D^{\dagger}=\begin{pmatrix} -0.172 & -0.074 & 0.122 & 0.231 & 0.239 & 0.194 & 0.156 & -0.010 \\ 0.057 & -0.019 & -0.106 & -0.022 & 0.041 & 0.048 & -0.227 & 0.887 \\ -0.229 & -0.310 & -0.246 & -0.063 & 0.055 & 0.108 & 0.022 & 0.102 \end{pmatrix} \tag{3}$$

Error analysis of the inverse Dower transformation

In Eq. (2) above, VCG was calculated from ECG in a noise-free situation as $\hat{S}_{vcg}=D^{\dagger}S_{ecg}$.

In the presence of a noise component ν, assumed to have zero-mean and being uncorrelated to S_{ecg} and S_{vcg}, the computation gives:

$$\hat{S}_{vcg}=D^{\dagger}\left(S_{ecg}+\nu_{ecg}\right)=S_{vcg}+D^{\dagger}\nu_{ecg}$$

The influence of ν on the calculated VCG can be analyzed statistically by looking at the expected value of $\hat{S}_{vcg}$:

$$\mathcal{E}\left\{\hat{S}_{vcg}\right\}=\mathcal{E}\left\{S_{vcg}+D^{\dagger}\nu_{ecg}\right\}=S_{vcg}+D^{\dagger}\mathcal{E}\left\{\nu_{ecg}\right\}=S_{vcg}$$

Numerically, the influence of ν is determined by the matrix $D^{\dagger}$. The maximum error of ν_{ecg} is found parallel to the vector corresponding to the largest singular value of $D^{\dagger}$. The singular values are:

$$\sigma=\begin{pmatrix} 0.938 \\ 0.531 \\ 0.396 \end{pmatrix}$$

The variance of $\hat{S}_{vcg}$may be analyzed as:

$$\mathcal{E}\left\{\hat{S}_{vcg}\hat{S}_{vcg}^{T}\right\}=S_{vcg}S_{vcg}^{T}+D^{\dagger}\mathcal{E}\left\{\nu_{ecg}\nu_{ecg}^{T}\right\}D^{\dagger T}$$

In the case of uncorrelated, equally distributed, measurement disturbances, the numerical influence of ν is determined by the matrix $D^{\dagger}D^{\dagger T}$ which has the singular values:

$$\sigma=\begin{pmatrix} 0.880 \\ 0.282 \\ 0.157 \end{pmatrix}$$

Least-squares minimization of residuals

In order to quantify the differences between the VCG signal, S_{vcg}, and the dVCG-signal, S_{dvcg}, for each lead the residual was calculated as:

$$S_{res}=S_{vcg}-\left(\alpha S_{dvcg}+\beta\right) \tag{4}$$

where α and β are parameters for scaling and offset of S_{dvcg} to minimize the residual [9].

Numerical values of α and β were found by using the MATLAB function `fminsearch` to minimize the function:

$$f(\alpha,\beta)=\sum_{i=1}^{n}(S_{\text{res}}(i))^2$$

where n is the length of the P-waves and S_{res} is calculated as Eq. (4) above. As an initial value of the parameters, (1,0) was chosen in all cases.

The magnitude of the residual was then calculated, for each lead, using the 2-norm of the residual divided by the 2-norm of the recorded VCG:

$$\text{Residual magnitude}=\frac{\sqrt{\sum_{i=1}^{n}|S_{\text{res}}(i)|^2}}{\sqrt{\sum_{i=1}^{n}|S_{\text{vcg}}(i)|^2}}$$

where S_{res} is the minimized residual in Eq. (4), S_{vcg} the P-wave of the recorded Frank-lead and n the length of the P-wave.

References

[1] Haïssaguerre M, Marcus FI, Fischer B, Clémenty J. Radiofrequency catheter ablation in unusual mechanisms of atrial fibrillation: report of three cases. J Cardiovasc Electrophysiol 1994;5:743—51.

[2] Platonov PG, Carlson J, Ingemansson MP, Roijer A, Chireikin LV, Olsson SB. Detection of inter-atrial conduction defects with unfiltered signal-averaged P wave ECG in patients with lone atrial fibrillation. Europace 2000;2:32—41.

[3] Platonov PG, Mitrofanova LB, Chireikin LV, Olsson SB. Morphology of inter-atrial conduction routes in patients with atrial fibrillation. Europace 2002;4:183—92.

[4] Xia Y, Hertervig E, Kongstad O, et al. Deterioration of interatrial conduction in patients with paroxysmal atrial fibrillation: electroanatomic mapping of the right atrium and coronary sinus. Heart Rhythm 2004;1:548—53.

[5] Edenbrandt L, Pahlm O. Vectorcardiogram synthesized from a 12-lead ECG: superiority of the inverse Dower matrix. J Electrocardiol 1988;21:361—7.

[6] Goldberger AL, Amaral LAN, Glass L, et al. PhysioBank, PhysioToolkit, and PhysioNet: components of a new research resource for complex physiologic signals. Circulation 2000;101:e215—20. Circulation electronic pages: <http://circ.ahajournals.org/cgi/content/full/101/23/e215>.

[7] Daskalov IK, Dotsinsky IA, Christov II . Developments in ECG acquisition, preprocessing, parameter measurement, and recording. IEEE Eng Med Biol Mag 1998;17:50—8.

[8] Dower GE, Machado HB, Osborne JA. On deriving the electrocardiogram from vectorcardiographic leads. Clin Cardiol 1980;3:87—95.

[9] Johansson R. System modeling and identification. Englewoods Cliffs, NJ: Prentice Hall; 1993 [Chapter 5].